A coordinated control of hybrid ac/dc microgrids with PV-wind-battery under variable generation and load conditions

Hu, Jiefeng; Shan, Yinghao; Xu, Yinliang; Guerrero, Josep M.

Published in:
International Journal of Electrical Power and Energy Systems

DOI (link to publication from Publisher):
10.1016/j.ijepes.2018.07.037

Publication date:
2019

Document Version
Early version, also known as pre-print

A Coordinated Control of Hybrid AC/DC Microgrids with PV-Wind-Battery under Variable Generation and Load Conditions

Jiefeng Hu [a], Yinghao Shan [a], and Josep M. Guerrero [b]
[a] J. Hu and Y. Shan are with Department of Electrical Engineering, The Hong Kong Polytechnic University. [b] J. M. Guerrero is with Department of Energy Technology, Aalborg University, Denmark.

Abstract— **Traditional power generation and consumption are undergoing major transformation. One of the tendency is to integrate microgrids into the distribution network with high penetration of renewable energy resources. This paper proposes a coordinated control strategy for a microgrid with hybrid energy resources and ac/dc loads. First, local-level coordinated control strategy of distributed converters is presented, where a model predictive power and voltage control (MPPVC) method is developed for the ac/dc interlinking converter to provide high quality voltages and to ensure smooth power transfer between the dc and ac subgrids. Meanwhile, smooth grid synchronization and connection can be achieved. After that, a system-level energy management scheme (EMS) is designed to ensure stable operation under variable power generation and consumption conditions. Simulation studies based on a 3.5 MW system demonstrate the effectiveness of the proposed control strategy.**

Index Terms—**Hybrid ac/dc microgrids, energy storage, coordinated control**

I. Introduction

In the last few years, due to the presence of dc power sources in microgrids such as PV, fuel-cell, energy storages, modern dc loads, and considering the existing century-long ac power systems, interests on hybrid ac/dc microgrids are growing rapidly [1], [2]. However, such configurations involve critical technical issues. Because of the intermittent nature of renewable energy, energy storage systems are critical part to absorb excessive energy during peak generation periods and compensate the insufficient power during peak load periods [3], [4].

The control and optimization of a hybrid ac/dc network are still open problems. In [5], a wind/hydrogen/supercapacitor hybrid power system was proposed to coordinate different sources to make the power injected into the grid controllable. In this dc-coupled system, all the energy sources are connected to a common dc bus before being connected to the grid through a main inverter. The impact of variable load demand on the system, however, is not studied. Another microgrid structure composed of PV array and fuel cell was proposed in [6]. A coordinated operation of unit-power control and feeder-flow control was developed to enhance system stability and reduce the number of operating mode changes. A similar microgrid configuration was presented in [7]. In this work, a coordinated strategy for the battery, wind generator, and dc load management was proposed for variations of wind power generation and load. Hybrid ac/dc structures where both dc bus and ac bus are connected with distributed generation and loads have also been investigated [8].

Compared to grid-connected mode, autonomous operation faces far more challenges. The key question is how to ensure the supply-demand balance within the microgrid. In [9], a hybrid ac/dc microgrid that can operate in grid-tied or islanded modes was proposed. In islanded mode, the main ac/dc interlinking converter is controlled to provide a stable voltage and frequency for the ac subgrid while the dc-link voltage is maintained by the bidirectional dc-dc converter. In grid-connected mode, the ac/dc interlinking converter is used to maintain a stable dc-link voltage and to exchange power between the microgrid and the utility system. Since then, similar hybrid ac/dc microgrid configurations and converters coordinated control schemes have been proposed to achieve different control objectives [10]-[13]. The practical fluctuation nature of renewable energy resources, however, are not considered in these literatures.

Recently, some research efforts have been made to develop more advanced energy management strategies. For example, energy management and control system are developed for a wind-pv-battery based microgrid [14]-[16]. It provides stable operation of the control in all microgrid subsystems under various power generation and load conditions. In [17], a distributed coordination control method for multiple bidirectional power converters interlinking the ac and dc subgrids was developed. A modular energy management system (EMS) based on mixed-integer linear programming is proposed in [18]. It can minimize the operating costs and promote self-consumption based on 24-hour ahead forecast data in a hybrid PV-wind-battery microgrid. Despite efforts that have been made, there are still technical issues need to be addressed before we can fully enjoy the benefits of such hybrid microgrids as follows.

First, in the control of ac/dc interlinking converter, all the methods mentioned above typically consist of an outer voltage loop and an inner current loop with proportional-integral-derivative (PID) controllers. This structure requires complicated coordinate transformation and much tuning effort is needed. Second, the existing EMSs are designed based on either grid-connected or islanded mode. Yet, comprehensive EMSs considering different operating conditions have not been put forward. Third, grid synchronization and connection are seldom mentioned. Without smooth grid synchronization and connection, power quality and system stability may be deteriorated.

In light of these, this paper aims to fill the above technical gaps. A coordinated control strategy is developed to control the distributed power converters in microgrid applications. It aims to ensure stable operation with high voltage quality under different operation modes and various generation and consumption conditions.

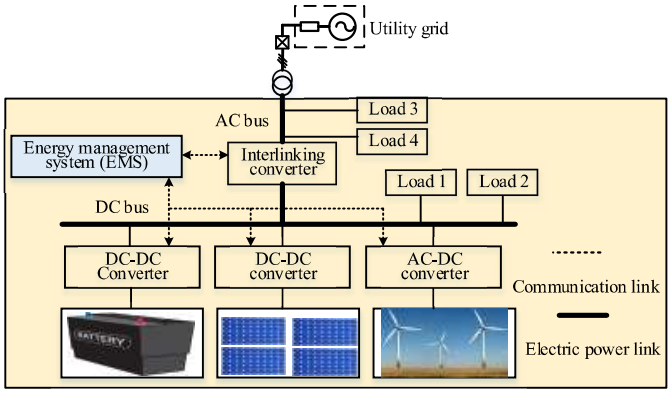

Fig. 1 A typical hybrid ac/dc microgrid.

II. Problems Identification and Control Objectives

Fig. 1 shows a hybrid ac/dc microgrid. Solar PV arrays and wind generators are connected to the common dc bus through power electronic converters. Energy storage system (ESS) is connected to the same dc bus via a dc/dc converter. The ac and dc buses are interconnected through a bidirectional ac/dc interlinking converter. Variable dc and ac loads are connected to the dc and ac buses, respectively. The control center collects the real-time information of the microgrid via the communication link, and then delivers back the control commands to control the converters to regulate the power flow in the electric power link.

Control of microgrids with various distributed generations (DGs) and loads has always been challenging. Unlike the conventional power plant, the renewable power generation does not provide continual electricity output. Take the solar PV for example, usually maximum solar irradiation occurs at midday while the demand is not high for residential loads. On the other hand, the peak demand occurs at evening when there is no generation from PV systems. With high level penetration of renewable energy, the usual peak production time and peak consumption time do not coincide. This characteristic will affect the system stability and degrade the overall system performance. For a hybrid ac/dc microgrid, the common dc-bus voltage and ac-bus voltage must be well maintained with a limited variation. This requires advanced control strategies. To be specifically, the main tasks to be fulfilled in this work can be described as follows.

At the local level, the power converters as the electronic interfaces between the energy resources and the common voltage buses should be controlled properly to inject power into the microgrid system. This will be achieved essentially by controlling the voltages and currents of the power converters.

At the system level, the power within the microgrid under various generation and loads should be balanced so that stable operation of the system can be achieved. With this goal, an EMS on top will be designed, based on which the operation modes of each power converter will be determined in a coordinated manner.

III. System Modelling

The mathematical models of the PV, wind and energy storage systems are essential requirements for the control technique development. These models are now well-known but for completeness they are described in details as follows.

A. Modeling of PV System

The PV system is shown in Fig. 2. The PV array is connected to the common dc bus through a boost converter. The solar modules are connected in series to form strings that are further connected in parallel as an array. The mathematical model of the solar module with its output current and output voltage has been well derived in [19]. Fig. 3 shows the output characteristic of a SunPower Spr-305E-WHT-D solar module. It can be seen that, under different solar irradiance and temperature, the maximum power points of the power-voltage curves are associated with different output voltages. Also, under certain solar irradiance, the output of the PV panel is varying with different terminal voltages. Therefore, in order to achieve maximum power point tracking (MPPT), the PV output voltage needs to be adjusted properly. This can be achieved by controlling the boost dc-dc converter.

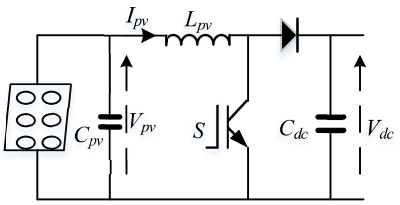

Fig. 2 PV system configuration.

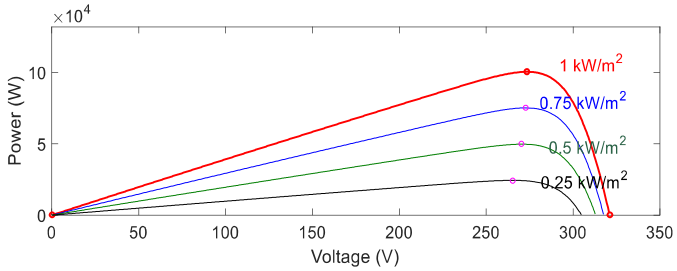

Fig. 3 Output characteristics of a solar module.

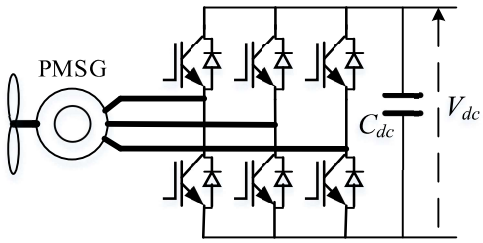

Fig. 4 Wind power system structure.

B. Modeling of Wind Turbine System

Fig. 4 shows the structure of the wind turbine system. The power captured by the wind turbine is given by [20]

$$P_m = 0.5\rho A C_p v_w^3 \tag{1}$$

where P_m is the mechanical output power of the turbine; C_p is the power coefficient of the turbine, which is a function of the tip-speed ratio (λ) and the pitch angle (β). ρ is the air density (kg/m^3); A is the turbine swept area (m^2); v_w is wind speed (m/s). The tip-speed ratio is given by

$$\lambda = \frac{R\omega_m}{v_w} \tag{2}$$

where R is the radius of the blade and ω_m is the turbine shaft speed in radians per second. For a given pitch angle, there is only one optimal value of λ that results in maximum C_p. Therefore, it is necessary to keep the shaft speed at an optimum value so as to produce maximum P_m under a certain wind speed. When the wind turbine spins, it drives the permanent magnet synchronous

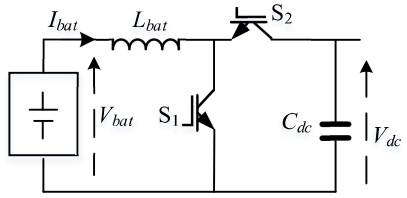

Fig. 5 Energy storage system.

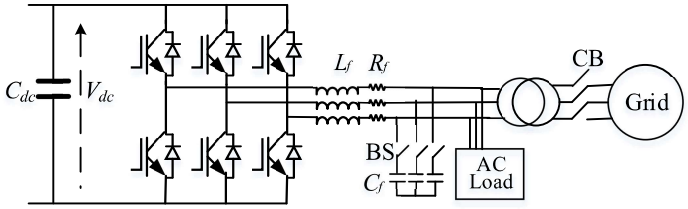

Fig. 6 AC side of the microgrid.

generator (PMSG) so that three-phase ac voltage will be induced at the stator windings. It is noted that the optimal generator T_e- ω_r curve can be obtained based on the optimal turbine P_m- ω_m characteristic, where T_e is the generator electromagnetic torque and ω_r is the rotor speed. The dynamic equation of the PMSG can be expressed as [12]

$$\begin{cases} \dfrac{di_{sd}}{dt} = -\dfrac{R_s}{L_d} i_{sd} + \dfrac{L_q}{L_d} p\omega_r i_{sq} + \dfrac{v_{sd}}{L_d} \\ \dfrac{di_{sq}}{dt} = -\dfrac{R_s}{L_q} i_{sq} - \dfrac{L_d}{L_q} p\omega_r i_{sd} - \dfrac{1}{L_q} p\omega_r \Phi_v + \dfrac{v_{sq}}{L_q} \end{cases} \tag{3}$$

where v_{sd} and v_{sq} are the d-q components of the stator voltage; i_{sd} and i_{sq} are the d-q components of stator current; L_d and L_q are the d-q components of the stator inductance. R_s is the stator winding resistance. Φ_v is the magnetic flux linkage. p is the number of pole pairs. The PMSG stator is then connected to the dc-bus through electronic interface. For small wind turbine system, a diode rectifier and a chopper with only one active switch are usually used. For high power applications, voltage source PWM converter is commonly utilized.

C. Modeling of ESS

Fig. 5 depicts the ESS structure. Due to the intermittent nature of renewable energy resources and the fluctuating load demand, ESS are vital to smooth the gap between the generation and consumption. Two important parameters to represent a battery are terminal voltage and state of charge (SOC) as [21]

$$V_{bat} = V_o + R_{bat} I_{bat} - \frac{KQ_{bat}}{Q_{bat} + \int I_{bat} dt} + A_{bat} \exp\left(B_{bat} \int I_{bat} dt\right) \tag{4}$$

$$SOC = 100\left(1 + \frac{\int I_{bat} dt}{Q_{bat}}\right) \tag{5}$$

where R_{bat} is internal resistance of the battery, V_o the open circuit voltage of the battery, I_{bat} the battery charging current, K the polarization voltage, Q_{bat} the battery capacity, A_{bat} the exponential voltage, and B_{bat} the exponential capacity. By controlling the bidirectional dc-dc converter, charging or discharging of the battery can be achieved.

D. Modeling of the AC Subgrid

Fig. 6 describes the ac side of the microgrid. In grid-connected mode, the circuit breaker (CB) is turned ON and the bypass switch

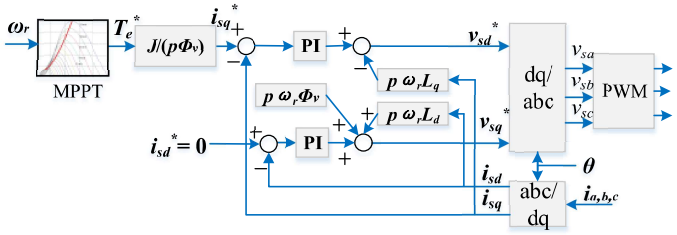

Fig. 7 Control scheme of the wind turbine system.

(BS) is switched OFF. The mathematical model can be expressed as

$$\boldsymbol{V}_i = \boldsymbol{V}_g + \boldsymbol{I}_f R_f + L_f \frac{d\boldsymbol{I}_f}{dt} \tag{6}$$

where $\boldsymbol{V}_i$ and $\boldsymbol{V}_g$ are the converter voltage vector and the grid voltage vector respectively; $\boldsymbol{I}_f$ the inductor current vector; L_f the filter inductance; R_f the equivalent resistance. The output active and reactive powers of the ac/dc interlinking converter are

$$P = \frac{3}{2}\mathrm{Re}\left\{\boldsymbol{V}_g \boldsymbol{I}_f^*\right\} = \frac{3}{2}\left(V_{g\alpha} I_{f\alpha} + V_{g\beta} I_{f\beta}\right) \tag{7}$$

$$Q = \frac{3}{2}\mathrm{Im}\left\{\boldsymbol{V}_g \boldsymbol{I}_f^*\right\} = \frac{3}{2}\left(V_{g\beta} I_{f\alpha} - V_{g\alpha} I_{f\beta}\right) \tag{8}$$

In islanded operation, the CB is turned OFF and the BS is switched ON. In this case, the dynamic behavior of the capacitor of the LC filer can be expressed as

$$C\frac{d\boldsymbol{V}_c}{dt} = \boldsymbol{I}_f - \boldsymbol{I}_L \tag{9}$$

where $\boldsymbol{V}_c$ is the capacitor voltage vector (i.e. the load voltage vector), C_f is the filter capacitance, $\boldsymbol{I}_L$ is the load current vector. The mathematical model of the ac/dc interlinking converter can be described as

$$\boldsymbol{V}_i = \boldsymbol{I}_f R + L\frac{d\boldsymbol{I}_f}{dt} + \boldsymbol{V}_c \tag{10}$$

IV. Local Level Control

A. Control of Boost Converter for PV

As explained in the previous section, in order to generate maximum power from the PV panel under various irradiance, the output voltage needs to be adjusted by controlling the boost dc-dc converter. Since the MPPT techniques of solar PV power generations have been widely developed and it is out of the scope of this work, it will not be investigated here. In this paper, an incremental conductance method is used to track the maximum power point [22]. Notice that the boost converter can be operated in on-MPPT or off-MPPT, which is determined according to the power balance of the system and the SOC of the battery, which will be explained further.

B. Control of AC/DC Converter for PMSG

To extract maximum power from the wind energy, a control scheme without wind-speed sensor (anemometer) is used here. Fig. 7 illustrates the control algorithm. The generator torque reference is obtained from the optimal T_e- ω_r curve according to the rotor speed. The q component of the stator current will then be calculated from inertia, pole pairs and magnetic flux linkage. After that, the stator voltage reference (i.e., required converter voltage) will be obtained according to (3) through PI control. The acceleration or deceleration of the generator is determined by the

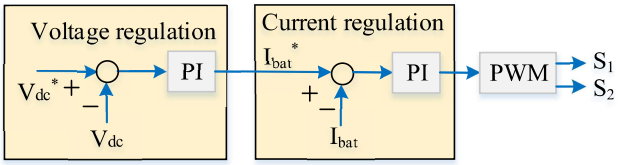

Fig. 8 Control of the ESS.

difference of the turbine torque and generator torque. If the generator speed is less than the optimal speed, the turbine torque is larger than the generator torque, and the generator will be accelerated. On the contrast, the generator will be decelerated if the generator speed is higher than the optimal speed. Therefore, the turbine and generator torques settle down to the optimum torque point at any wind speed, and the wind turbine is operated at the maximum power point. Similar to the solar PV system, the wind generator can be operated in on-MPPT or off-MPPT, which is determined according to the power balance of the system and the SOC of the battery.

C. Control of DC/DC Converter for ESS

The block diagram of the ESS control is illustrated in Fig. 8. The charging/discharging current reference is compared with the measured current. The error is delivered to a PI controller. If the ESS is used to maintain the dc-bus voltage, then a two-loop control scheme should be adopted [13]. The error between the measured dc-bus voltage and the reference voltage is set as the input of the PI controller and the output is the reference current for the inner current loop. For instance, when the dc bus voltage is greater than the reference voltage, the outer voltage controller generates a negative current reference. The inner current loop then adjusts the duty cycle to force the current flow from the dc bus to the battery, which results in charging the battery. Subsequently, the dc bus voltage decreases to the reference as the excess energy is absorbed by the battery. It is noted that the SOC limits and the charging/discharging rates should be considered as the energy constraints of the battery

$$10\% \le SOC \le 90\% \tag{11}$$

$$-\frac{P_{Bat\_N}}{V_{Bat}} \le I_{bat} \le \frac{P_{Bat\_N}}{V_{Bat}} \tag{12}$$

where P_{Bat_N} is the battery rated power; V_{Bat} the normal voltage.

D. Control of AC/DC Interlinking Converter

The major contribution of this work is to develop a MPPVC approach for the ac/dc interlinking converter for microgrid applications. Fig. 9 shows the block diagram. To be specifically, a model predictive power control (MPPC) in grid-connected mode and a model predictive voltage control (MPVC) for islanded mode and grid synchronization will be developed.

In grid-connected mode, the ac/dc interlinking converter is used to maintain a stable dc-bus voltage for dc loads and to exchange power between the microgrid and the utility system. The active power reference is obtained from the outer voltage loop where the PI control is used to regulate the dc-bus voltage. When resource conditions or load capacities change, the dc bus voltage is adjusted to constant so as to keep the power balance within the system. After the power references are obtained, the system model is used to predict the powers at next sampling instant. A cost function is then employed as the criterion to select the optimum voltage vector of the converter. Finally, the voltage vector that can minimize the cost function is applied. In MPPC, the active and reactive powers

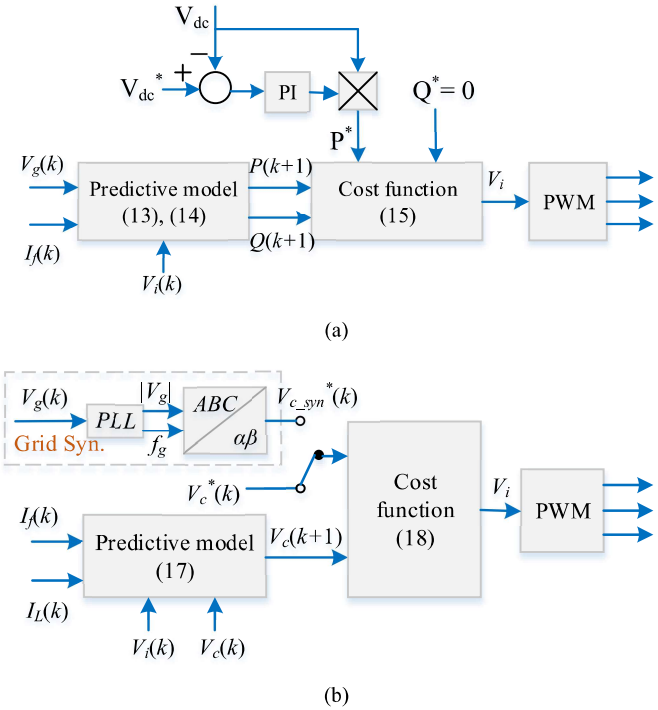

Fig. 9 Proposed control for interlinking converter, (a) MPPC, (b) MPVC.

at the end of a sampling period can be predicted from (6), (7) and (8) as

$$P^{k+1} = T_s\left[-\frac{R}{L}P^k - \omega Q^k + \frac{3}{2L}\left(\left|\boldsymbol{V}_g\right|^2 - \mathrm{Re}\left(\boldsymbol{V}_g\boldsymbol{V}_i^*\right)\right)\right] + P^k \tag{13}$$

$$Q^{k+1} = T_s\left[\omega P^k - \frac{R}{L}Q^k - \frac{3}{2L}\mathrm{Im}\left(\boldsymbol{V}_g\boldsymbol{V}_i^*\right)\right] + Q^k \tag{14}$$

where ω is the grid frequency in radians. Since the control objectives in grid-tied mode are the active and reactive powers. Therefore, we can evaluate the effects of each voltage vector on P and Q and select the one minimizing the following cost function

$$J_P = \left(P_{ref} - P^{k+1}\right)^2 + \left(Q_{ref} - Q^{k+1}\right)^2 \tag{15}$$

In islanded operation, the dc-bus voltage can be maintained by the ESS, while the ac/dc interlinking converter acts as a voltage source to provide a stable ac voltage for the ac load. With this goal, the capacitor voltage should be the control objective of the MPVC controller. Combining (9) and (10), the system model can be rewritten as a state-space system

$$\frac{d\boldsymbol{x}}{dt} = A\boldsymbol{x} + B\boldsymbol{y} \tag{16}$$

where

$$\boldsymbol{x} = \begin{bmatrix}\boldsymbol{V}_c \\ \boldsymbol{I}_f\end{bmatrix}, \quad \boldsymbol{y} = \begin{bmatrix}\boldsymbol{V}_i \\ \boldsymbol{I}_L\end{bmatrix}, \quad A = \begin{bmatrix}0 & 1/C_f \\ -1/L_f & -R_f/L_f\end{bmatrix},$$

$$B = \begin{bmatrix}0 & -1/C_f \\ 1/L_f & 0\end{bmatrix},$$

By solving the linear differential equation of (16), it can be expressed in discrete-time form as

$$\boldsymbol{x}(k+1) = e^{T_s A}\boldsymbol{x}(k) + A^{-1}(e^{T_s A} - \boldsymbol{I}_{2\times 2})B\boldsymbol{y}(k) \tag{17}$$

Therefore, the capacitor voltage at (k+1)th instant can be predicted according to (17). To control the capacitor voltage tightly, the cost function is formulated to

$$J_V = \left(V_{c\alpha}^{ref} - V_{c\alpha}^{k+1}\right)^2 + \left(V_{c\beta}^{ref} - V_{c\beta}^{k+1}\right)^2 \tag{18}$$

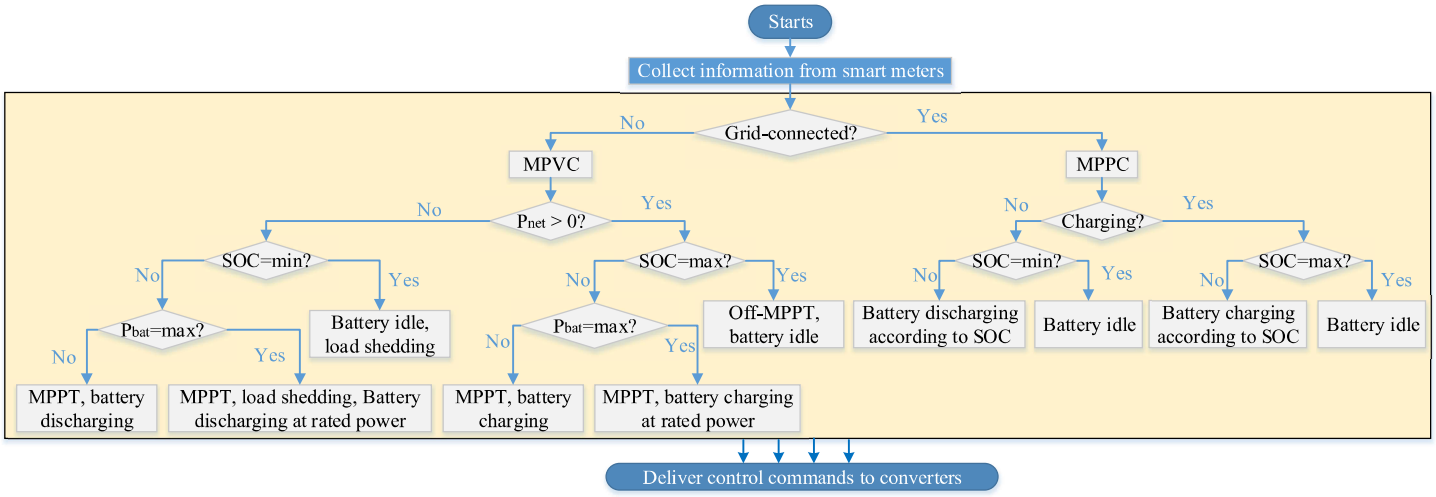

Fig. 10 Comprehensive EMS – System level control.

where $V_{c\alpha}$ and $V_{c\beta}$ are the real and imaginary components of the capacitor voltage vector, respectively. Based on this cost function, the voltage vector that generates the least value of J_V will be applied during the next sampling period. Because the α and β components are tightly controlled, the $\boldsymbol{V}_c$ can track its reference. Thus stable and sinusoidal voltage can be established.

In Grid synchronization, phase-locked loop (PLL) is used to obtain the grid voltage amplitude and frequency. Then, a voltage with the same amplitude and slightly lower frequency as the grid voltage is set as the reference voltage for the cost function (18). In this way, the microgrid ac voltage phasor and grid voltage phasor will rotate in different angular speeds but with same amplitudes. Once the phase angle of the microgrid ac voltage is aligned with that of the grid voltage, grid connection can be conducted.

V. System Level Control

In this section, the system level control is developed. The overall control logic diagram is illustrated in Fig. 10. For a hybrid ac/dc microgrid, there must be a number of operation modes that need to be considered in order to ensure reliable power supply. The power within the microgrid should be balanced as follows

$$P_{pv} + P_w + + P_{bat} + P_g - P_{loss} = P_{acL} + P_{dcL} \tag{19}$$

where P_{bat} is the battery power; P_{loss} the total power loss; P_g the power exchange with utility. Positive P_{bat} indicates discharging while negative represents charging. Positive P_g means drawing power from utility whereas negative indicates injecting power to utility. P_{net} is defined as P_{pv} and P_w subtracted by P_{acL}, P_{dcL} and P_{loss}.

A. Mode 1 operation

This mode refers to grid-connected operation. Any power surplus or deficit within the microgrid is automatically balanced by the ac distribution network. In this case, the PV and wind generator should produce as much power as possible for the microgrid and the utility. Also, no load shedding is required and the ESS can be charged or discharged by using closed current loop control. The ac/dc interlinking converter operates in MPPC scheme to maintain the dc-bus voltage to transfer the power between the dc subgrid and ac subgrid.

B. Mode 2 operation

This mode refers to islanded operation. Since the hybrid microgrid becomes an isolated system, the power needs to be balanced within the microgrid. In this case, the dc-bus voltage is maintained by the ESS using a two-loop control structure. The ac-bus voltage is established by the ac/dc interlinking converter using MPVC scheme. Specifically, there are two conditions that need to be considered.

1) Low wind and irradiation and heavy load

Under this scenario, the generation from PV and wind cannot meet the load demand. As a result, both the PV and wind generator should operate in MPPT while the ESS provides additional power by battery discharging. If the required power by the ESS exceeds the power rating of the battery or the SOC drops down to the minimum value, load shedding becomes necessary to guarantee power supply to the most critical loads.

2) High wind and irradiation and light load

Under this circumstance, the generation from PV and wind is greater than the load demand. The ESS is used to absorb the excessive energy by charging the battery. If the power absorbed by the battery exceeds the power rating of the battery or the SOC reaches the maximum value, Off-MPPT operation of the PV and wind systems are needed.

C. Mode 3 operation

This mode corresponds to grid synchronization and connection. Under this mode, the terminal voltage of the ac subgrid starts to track the utility voltage. When the voltages match each other, grid connection can be carried out. To a certain extent, this mode can be regarded as the extension of Mode 2. Similar to Mode 2, the dc-bus voltage relies on ESS and the ac-bus voltage is provided by the interlinking converter.

VI. Case Studies

The proposed hybrid microgrid shown in Fig. 1 is realized in MATLAB/Simulink. The system parameters are listed in Table I. Load 1 and 2 are linear loads represented by using constant resistances. Load 3 and 4 are modelled as a constant power type representing nonlinear load. Simulation studies are carried out in accordance with various conditions as follows:

Case 1) the microgrid is connected to utility grid with generation and load variations;

Case 2) islanded operation with various generation and loads;

Case 3) grid synchronization and re-connection.

TABLE I System Parameters

Description	Value
Solar PV	SunPower Spr-305E-WHT-D, 2 MW
Wind turbine	Base wind speed 12m/s, R=31m, C_p=0.47
PMSG	1.5 MW, L_d=L_q=0.3mH, Φ_V=1.48Wb, p = 48
ESS	Lithium-Ion battery, 1 MW, 300V, 1.3 kA·h
DC-bus voltage	1200 V
DC-bus capacitor	6 mF
AC-bus voltage	25 kV / 0.69 kV
AC-bus LC filter	L = 0.6mH, C=1338μF
Linear loads	Critical load 1 – 1MW, non-critical load 2 – 0.5MW
Non-linear loads	Critical load 3 – 1MW, non-critical load 4 – 0.5MW

TABLE II Events during Case 1 (grid-connected).

Events	Operations	Time (s)
1	Wind speed step down	5
2	Load 3 switched in	8
3	Load 2 switched in	11
4	Load 4 switched in	13
5	Wind speed step up	15
6	Load 1 switched in	17

TABLE III Events during Case 2 (islanded).

Events	Operations	Time (s)
1	Solar irradiation ramps up	5
2	Load 1 switched in	9
3	Solar irradiation ramps down	11
4	Load 2 and 4 switched in	11
5	Load 4 switched out (load shedding)	12

A. Case 1

Under grid-connected operation, both the PV and the wind generator should be operated in MPPT. The battery is kept being charged as the utility power is available. The solar irradiation level is kept constant at 600W/m^2, resulting in about 1.2MW power output. The wind speed steps down to 8m/s at 5s and steps up to 10m/s at 15s. Fig. 11 shows the performance of the wind power system. It can be seen that the rotor speed is controlled accordingly under such wind speed variation so that the PMSG generates maximum power output.

In order to demonstrate the effectiveness of the proposed control schemes and the reliable operation, a series of events have been imposed, as shown in Table II. The system performance in different operation events is shown in Fig. 12. Prior to Event 2, the power generated from PV and wind generator is partly stored by ESS while the excess is fed back to the utility. When Event 2 occurs, i.e., Load 3 is switched in, the microgrid started to draw power from utility grid because the power generated from PV and wind generators is slightly less than the demand from the load and the ESS. When the Load 2, 4 and 1 are switched in afterwards, the microgrid imports more power from utility accordingly. During the grid-connected operation, the voltage of the ac subgrid is fixed by the utility, while dc subgrid voltage is maintained successfully by the ac/dc interlinking converter using MPPC scheme.

B. Case 2

Compared to grid-connected operation, islanded mode is more challenging due to the unavailability of the utility system. Thanks to the proposed MPVC method and the EMS strategy, the microgrid is able to achieve stable operation and supply high quality electricity, as shown in the follows. In this test, wind speed is fixed at 10m/s, while the solar irradiation presents fluctuating feature. Initially, Load 3 (1MW non-linear load) is connected to the ac sugbrid. A variety of events is adopted afterwards, as listed in Table III.

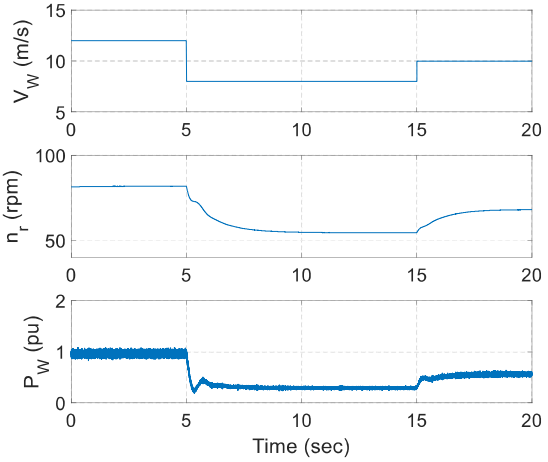

Fig. 11 PMSG performance under wind speed variation in Case 1.

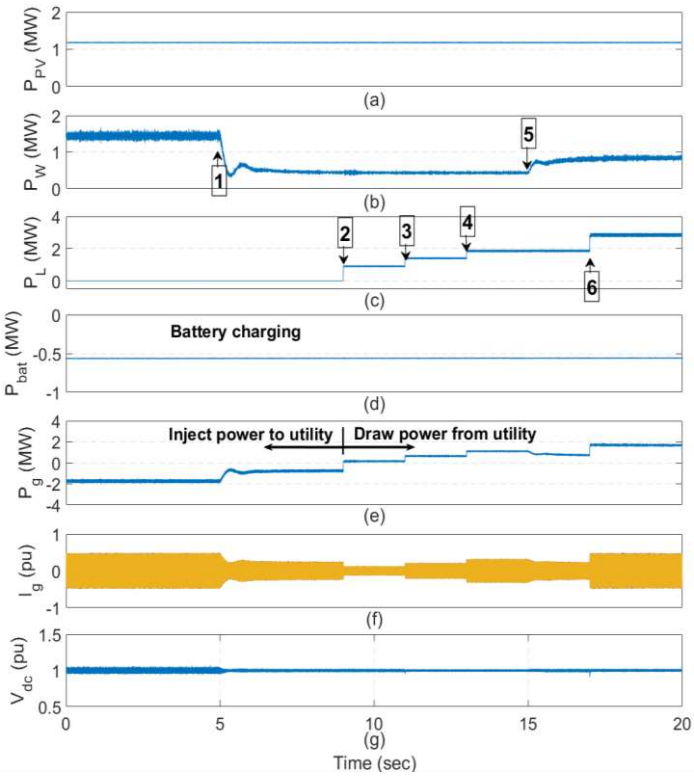

Fig. 12. Case 1 performance under variable wind power and load demand condition in grid-connected mode. The waveforms from top to bottom are (a) PV power, (b) wind power, (c) total load demand, (d) battery power, (e) power exchanged between micro and utility grid, (f) current flow between micro and utility grid, (g) dc-bus voltage.

Fig. 13 presents the response of the PV system. It can be observed that the boost converter successfully adjusts its duty ratio in order to change the PV output voltage, leading to maximum power output. Fig. 14 shows the comprehensive system performance of the microgrid. Before Event 3 and 4, the generation from PV and wind generator can fully meet the load demand. At 11s, Load 2 and 4 are switched in simultaneously and the PV output started to drop, resulting in ESS discharging to provide additional energy. Since the PV output is decreased gradually, the ESS increased its output accordingly to fill the gap between generation and consumption until it reached the maximum capacity at around 12s. After that, load shedding strategy is activated by switching out the non-critical Load 4.

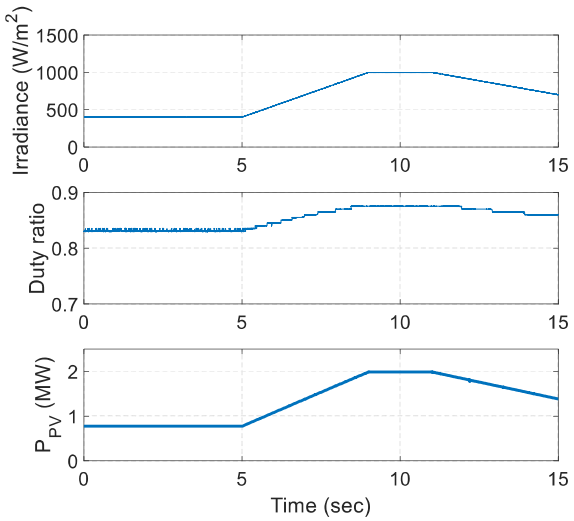

Fig. 13. PV output under variable solar irradiation in Case 2.

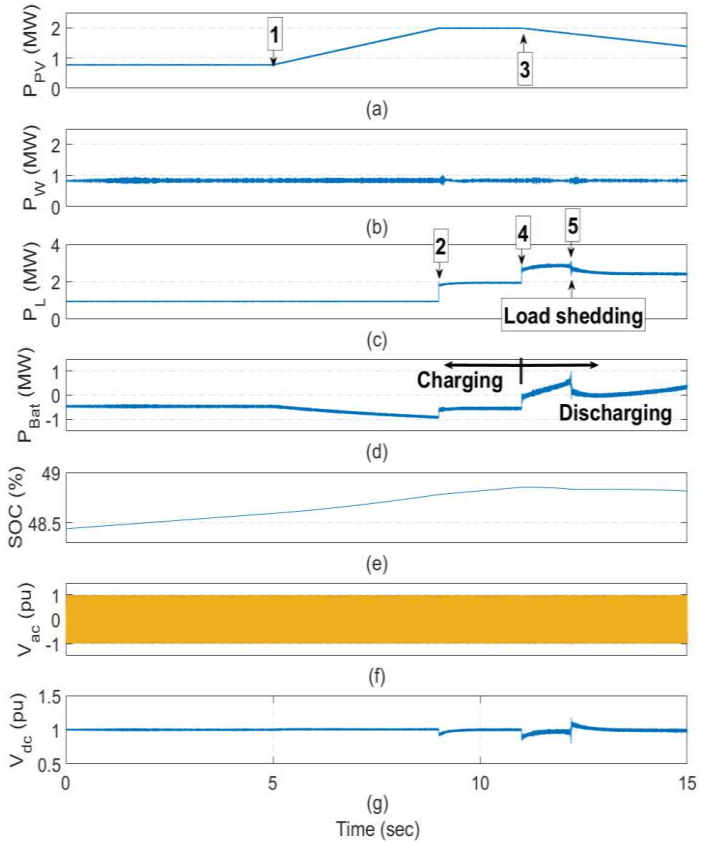

Fig. 14. Case 2 performance under variable PV power and load demand condition in islanded mode. The waveforms from top to bottom are (a) PV power, (b) wind power, (c) total load demand, (d) battery power, (e) SOC, (f) ac-bus voltage, (g) dc-bus voltage.

Since the ac-bus voltage is an important aspect to evaluate the microgrid performance in islanded operation, its zoom-in waveform is plotted out in Fig. 15(a) to obtain a better observation. It can be seen that the ac voltage is sinusoidal and well controlled using MPVC. Fig. 15(b) shows the FFT analysis. It is seen that the harmonic spectrum is clean with only 1.06% THD, indicating high voltage quality.

C. Case 3

Existing research seldom mentions the grid synchronization and connection of the hybrid ac/dc microgrids, but it will be studied

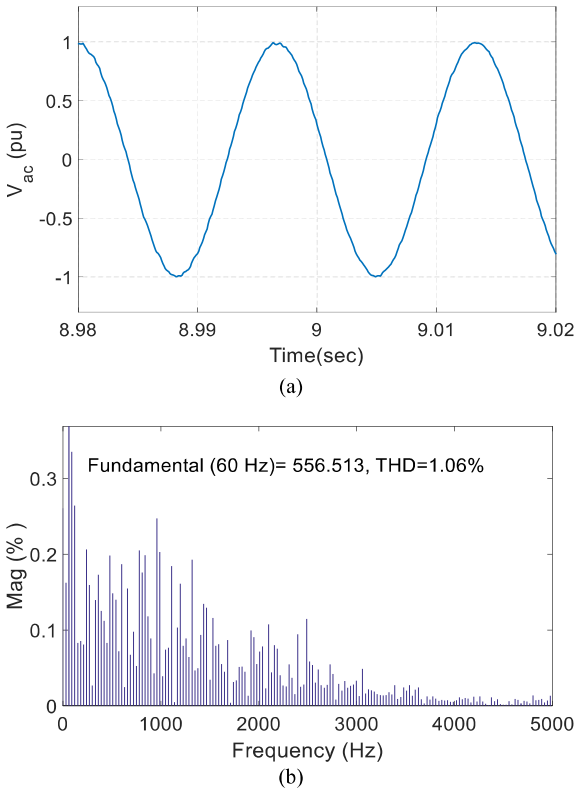

Fig. 15 AC-bus voltage in Case 2, (a) phase A voltage, (b) FFT analysis.

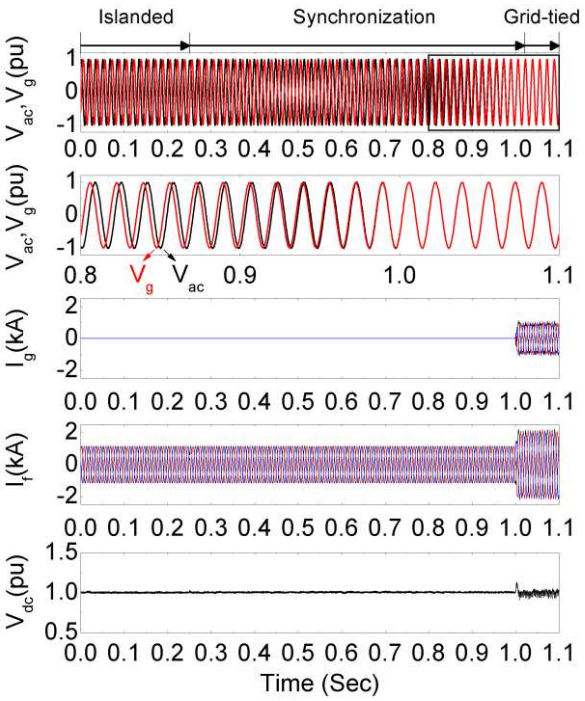

Fig. 16. Case 3 performance in grid synchronization and connection.

here. Fig. 16 shows the detailed results. Initially the microgrid operated at islanded mode. The grid synchronization algorithm starts to operate at 0.25s and the microgrid is connected to utility grid at 1s. It can be seen that the ac terminal voltage of the microgrid is able to track the utility grid voltage gradually and smoothly, while the dc-bus voltage can be maintained. It is also seen that no overshoots in grid current and inverter output currents are observed in the grid-connection transient. These prompts fast and smooth grid synchronization and connection operation.

VII. Conclusion

In this paper, a coordinated control strategy of hybrid ac/dc microgrid with PV-wind-battery sources is proposed. At the local level, the interfaced power converters are controlled coordinately to control the output voltage and current. Specifically, A model predictive power and voltage control(MPPVC) method is developed for the ac/dc interlinking converter to maintain stable ac/dc buses voltages and to facilitate the grid synchronization and connection. At the system level, an energy management scheme is developed to maintain the power balance under variable generation and consumption condition. Various case studies under grid-connected, islanded and grid synchronization modes have validated the satisfactory performance of the microgrid architecture and the proposed control strategy. The main contribution of this work can be summarized as follows.

References

[1] R. H. Lasseter, "Smart distribution: coupled microgrids", *IEEE Proceedings*, vol. 99, no. 6, 1074-1082, June 2011.

[2] X. Zhou, L. Zhou, Y. Chen, J. M. Guerrero, A. Luo, W. Xu, and L. Yang, "A microgrid cluster structure and its autonomous coordination control strategy," *Int J Electr Power Energy Syst,* vol. 100, pp. 69-80, 2018.

[3] D. E. Olivares, and et al, "Trends in microgrid control", *IEEE Trans. Smart Grid*, vol. 5, no. 4, 1905-1919, July 2014.

[4] M. Baharizadeh, H. R. Karshenas, and J. M. Guerrero, "An improved power control strategy for hybrid ac-dc microgrids," *Int J Electr Power Energy Syst,* vol. 95, pp. 364-373, 2018.

[5] T. Zhou and B. Francois, "Energy management and power control of a hybrid active wind generator for distributed power generation and grid integration", *IEEE Trans. Ind. Electron*., vol. 58, no. 1, 95-104, Jan. 2011.

[6] L. N. Khanh, J. J. Seo, Y. S. Kim, and D. J. Won, "Power-management strategies for a grid-connected PV-FC hybrid system", *IEEE Trans. Power Delivery*, vol. 25, no. 3, 1874-1882, Jul. 2010.

[7] L. Xu and D. Chen, "Control and operation of a dc microgrid with variable generation and energy storage", *IEEE Trans. Power Delivery*, vol. 26, no. 4, 2513-2522, Oct. 2011.

[8] H. Zhou, T. Bhattacharya, D. Tran, T. S. T. Siew, and A. M. Khambadkone, "Composite energy storage system involving battery and ultracapacitor with dynamic energy management in microgrid applications", *IEEE Trans. Power Electron*., vol. 26, no. 3, 923-930, Apr. 2017.

[9] X. Liu, P. Wang, and P. C. Loh, "A hybrid AC/DC microgrid and its coordination control", *IEEE Trans. Smart Grid*, vol. 2, no. 2, 278-286, June 2011.

[10] C. N. Bhende, S. Mishra, and S. G. Malla, "Permanent magnet synchronous generator-based standalone wind energy supply system", *IEEE Trans. Sustain. Energy*, vol. 2, no. 4, 361-373, Oct. 2011.

[11] P. C. Loh, D. Li, Y. K. Chai, and F. Blaabjerg, "Autonomous operation of hybrid microgrid with ac and dc subgrids", *IEEE Trans. Power Electron*., vol. 28, no. 5, 2214-2223, May 2013.

[12] P. C. Loh, D. Li, Y. K. Chai, and F. Blaabjerg, "Autonomous control of interlinking converter with energy storage in hybrid ac-dc microgrid", *IEEE Trans. Ind. Appl*., vol. 49, no. 3, 1374-1382, May/June 2013.

[13] P. Wang, C. Jin, D. Zhu, Y. Tang, P. C. Loh, and F. H. Choo, "Distributed control for autonomous operation of a three-port ac/dc/ds hybrid microgrid", *IEEE Trans. Ind. Electron*., vol. 62, no. 2, 1279-1290, Feb. 2015.

[14] A. Merabet, K. T. Ahmed, H. Ibrahim, R. Beguenane, and A. Ghias, "Energy management and control system for laboratory scale microgrid based wind-pv-battery," *IEEE Trans. Sustain. Energy,* vol. 8, no. 1, pp. 145–154, Jan. 2017.

[15] T. Ma, M. H. Cintuglu, and O. A. Mohammed, "Control of hybrid ac/dc microgrid involving energy storage and pulsed loads", *IEEE Trans. Ind. Appl*., vol. 53, no. 1, 567-575, 2017.

[16] J. Yang, W. Yuan, Y. Sun, H. Han, X. Hou, and J. M. Guerrero, "A novel quasi-master-slave control frame for pv-storage independent microgrid," *Int J Electr Power Energy Syst,* vol. 97, pp. 262–274, 2018.

[17] Y. Xia, Y. Peng, P. Yang, M. Yu, and W. Wei, "Distributed coordination control for multiple bidirectional power converters in a hybrid ac/dc microgrid", *IEEE Trans. Power Electron*., vol. 32, no. 6, 4949-4959, 2017.

[18] A. C. Luna, N. L. Diaz, M. Graells, J. C. Vasquez, and J. M. Guerrero, "Mixed-integer-linear-programming-based energy management system for hybrid pv-wind-battery microgrids: modeling, design, and experimental verification", *IEEE Trans. Power Electron*., vol. 32, no. 4, 2769-2783, Apr. 2017.

[19] G. M. Masters, "Renewable and efficient electric power systems", John Wiley & Sons, 2004.

[20] M. E. Haque, M. Negnevitsky, and K. M. Muttaqi, "A novel control strategy for a variable-speed wind turbine with a permanent-magnet synchronous generator", *IEEE Trans. Ind. Appl*., vol. 46, no. 1, 331-339, Jan./Feb. 2010.

[21] O. Tremblay, L. A. Dessaint, and A. I. Dekkiche, "A generic battery model for the dynamic simulation of hybrid electric vehicles", in *Proc. of IEEE Veh. Power Propulsion Conf.*, 2007, pp. 284-289.

[22] I. V. Banu, R. Beniuga, and M. Istrate, "Comparative analysis of the perturb-and-observe and incremental conductance MPPT methods", in *Proc. of Int. Symposium on Advanced Topics in Electrical Engineering*, 2013, pp. 1-4.